

Scaling behavior and positivity violation of the gluon propagator in full QCD

Patrick O. Bowman,¹ Urs M. Heller,² Derek B. Leinweber,³ Maria B. Parappilly,³ André Sternbeck,³ Lorenz von Smekal,³ Anthony G. Williams,³ and Jianbo Zhang⁴

¹*Centre of Theoretical Chemistry and Physics, Institute of Fundamental Sciences, Massey University (Auckland), Private Bag 102904, NSMSC, Auckland NZ*

²*American Physical Society, One Research Road, Box 9000, Ridge, NY 11961-9000, USA*

³*Special Research Center for the Subatomic Structure of Matter (CSSM), Department of Physics, University of Adelaide 5005, Australia*

⁴*Department of Physics, Zhejiang University, Hangzhou, Zhejiang 310027, P.R. China*

(Dated: March 23, 2007)

The Landau-gauge gluon propagator is studied using the coarse and fine dynamical MILC configurations. The effects of dynamical quarks are clearly visible and lead to a reduction of the nonperturbative infrared enhancement relative to the quenched case. Lattice spacing effects are studied and found to be small. The gluon spectral function is shown to clearly violate positivity in both quenched and full QCD.

PACS numbers: 12.38.Gc 11.15.Ha 12.38.Aw 14.70.Dj

I. INTRODUCTION

Quarks and gluons, which carry color charge, are not observed as free particles, but only inside the colorless bound states called hadrons. This phenomenon is called confinement. The gluon propagator has long been studied regarding confinement. It is also an important input for many phenomenological calculations in hadronic physics (see e.g. the reviews [1–5]).

In the last decade there have been many lattice studies devoted to the gluon propagator in the Landau gauge. Most of them are done either in quenched QCD [6–19] or in quenched $SU(2)$ [20–22], but there are also more recent reports [23–25] by us and others for the case of full QCD. All lattice studies so far have indicated that the gluon propagator in Landau gauge is infrared finite (see e.g. [13, 23, 26]). This, however, disagrees with the corresponding results obtained in studies of the Dyson-Schwinger equation (DSE) for the gluon propagator. There an infrared vanishing gluon propagator is predicted [1, 27, 28]. Such an infrared behavior has also been found using stochastic quantization [29] and in studies of exact renormalization group equations [30]. Recent DSE studies on a finite torus strongly suggest that this discrepancy is due to finite volume effects [31].

In this paper we extend the previous work reported in [23] to finer lattices studying the scaling behavior of the gluon propagator in Landau gauge. We show that the gluon Schwinger function in quenched and full QCD is negative in a certain interval. This is consistent with both a recent lattice study of two flavor QCD [26] and with results obtained in DSE studies [1, 32].

II. POSITIVITY OF EUCLIDEAN GREEN'S FUNCTIONS

Here, a note on positivity and its violation is in order. In quantum field theory in Minkowski space, if a cer-

tain degree of freedom is supposed to describe a physical asymptotic state, it must not have any negative norm contributions in its propagator. That is, the propagator must not violate positivity. Otherwise the states it describes cannot be part of the physical state space; they are, so to say, confined from the physical world.

Considering Euclidean Green's functions, positivity translates into the notion of reflection positivity as one of the famous Osterwalder-Schrader axioms of Euclidean quantum field theory. For our purpose it is instructive, and also sufficient, to consider reflection positivity in the case of an Euclidean 2-point function, $D(x - y)$, whose corresponding propagator in momentum space, $D(q^2)$, can be written in a spectral representation

$$D(q^2) = \int_0^\infty dm^2 \frac{\rho(m^2)}{q^2 + m^2} \quad (1)$$

where q^2 denotes the four-momentum squared in Euclidean space and m^2 is the mass squared. The spectral function, $\rho(m^2)$, is unknown in general, but if $\rho(m^2) \geq 0$ for all m^2 , Eq. (1) is known as the Källen-Lehmann representation.

The 1-dimensional Fourier transform of $D(q^2)$ at zero spatial momentum defines the wall-to-wall correlator [33]

$$C(t) = \int_0^\infty dm \rho(m^2) e^{-mt}. \quad (2)$$

In lattice spectroscopy the exponential decay of this function is used to extract the mass of a particle state.

Obviously, from Eq. (2), if the spectral function is positive, then $C(t) \geq 0$. This needs not to be the case the other way around. If, however, $C(t)$ is found to be negative, $\rho(m^2)$ cannot be a positive spectral function. That is, there is no Källen-Lehmann representation and the corresponding states cannot appear in the physical particle spectrum: they are confined.

Alternatively, an effective mass [6, 33]

$$m_{\text{eff}}(t) := -\frac{d}{dt} \ln C(t)$$

could be considered. For positive ρ , the slope of $m_{\text{eff}}(t)$ cannot be positive. If, on the contrary, $m_{\text{eff}}(t)$ increases with t , ρ cannot be a positive spectral function.

The gluon 2-point function was known from the beginning to violate positivity. Already in the first numerical study [6] of the gluon propagator in quenched lattice QCD in Landau gauge this has been demonstrated by an effective gluon mass rising with increasing distance t (see also [34–36]). A direct observation, however, of a non-positive gluon correlator, $C(t)$, in particular for full QCD, has been unfeasible for a long time. Nevertheless, in more recent times a non-positive $C(t)$ has been observed in studies of the corresponding Dyson-Schwinger equation [32], in quenched $SU(2)$ lattice gauge theory in three dimensions [37] and hinted at in QCD with dynamical quarks [38]. Explicit evidence in quenched and full QCD (clover-improved Wilson fermions) has been given recently in [26]. To complete those findings, in this paper we show that $C(t) < 0$ for some t in full QCD with 2+1 flavors of $\mathcal{O}(a^2)$ Symanzik-improved staggered fermions.

III. GLUON PROPAGATOR ON THE LATTICE

In the continuum, the Euclidean gluon propagator in Landau gauge has the tensor structure

$$D_{\mu\nu}(q) = \left(\delta_{\mu\nu} - \frac{q_\mu q_\nu}{q^2} \right) D(q^2). \quad (3)$$

Here $D(q^2)$ is a scalar function which contains the whole nonperturbative information of $D_{\mu\nu}(q)$. At tree-level

$$D(q^2) = \frac{1}{q^2}. \quad (4)$$

Assuming Eq. (3) to be well satisfied on the lattice, we have calculated $D(q^2)$ using a variety of quenched and dynamical configurations. These configurations were provided to us by the MILC collaboration [39] through the Gauge Connection [40] and were generated with the $\mathcal{O}(a^2)$ one-loop Symanzik improved gauge action [41]. For the dynamical configurations the “AsqTad” quark action was used. This is an $\mathcal{O}(a^2)$ Symanzik-improved staggered fermion action with 2+1 flavors implemented using the “fourth-root trick”. The lattice spacing was determined from the variant Sommer parameter, r_1 [39]. Following MILC convention we refer to the $28^3 \times 96$ configurations as being “fine” lattices and the $20^3 \times 64$ configurations as the “coarse” lattices. See Table I for details.

With this lattice gauge action the Landau-gauge gluon propagator at tree-level is

$$D^{-1}(p_\mu) = \frac{4}{a^2} \sum_\mu \left\{ \sin^2 \left(\frac{p_\mu a}{2} \right) + \frac{1}{3} \sin^4 \left(\frac{p_\mu a}{2} \right) \right\}, \quad (5)$$

TABLE I: Lattice parameters used in this study. The dynamical configurations each have two degenerate light quarks (up/down) and a heavier quark (strange). In the table we show the sea quark masses both in dimensionless (lattice) units and estimated physical units. For details see Ref. [39].

	Dimensions	β	a (fm)	ma	m (MeV)	#Config.
1	$28^3 \times 96$	8.40	0.086	— quenched —	—	150
2	$28^3 \times 96$	7.09	0.086	0.062, 0.031	14, 68	108
3	$28^3 \times 96$	7.11	0.086	0.124, 0.031	27, 68	110
4	$20^3 \times 64$	8.00	0.120	— quenched —	—	192
5	$20^3 \times 64$	6.76	0.121	0.010, 0.050	16, 82	203
6	$20^3 \times 64$	6.79	0.120	0.020, 0.050	33, 82	249
7	$20^3 \times 64$	6.81	0.120	0.030, 0.050	49, 82	268
8	$20^3 \times 64$	6.83	0.119	0.040, 0.050	66, 83	318

where

$$p_\mu = \frac{2\pi n_\mu}{aL_\mu}, \quad n_\mu \in \left(-\frac{L_\mu}{2}, \frac{L_\mu}{2} \right], \quad (6)$$

a is the lattice spacing and L_μ is the length of the lattice in the μ direction. To ensure the correct tree-level behavior for the lattice gluon propagator, a “kinematic” choice of momentum,

$$q_\mu(p_\mu) \equiv \frac{2}{a} \sqrt{\sin^2 \left(\frac{p_\mu a}{2} \right) + \frac{1}{3} \sin^4 \left(\frac{p_\mu a}{2} \right)}. \quad (7)$$

is employed [13].

Lattice Monte Carlo estimates for the bare gluon propagator, $D(q^2)$, have to be renormalized. The renormalized propagator $D_R(q^2; \mu^2)$ is related to $D(q^2)$ through

$$D(q^2) = Z_3(\mu^2, a) D_R(q^2; \mu^2) \quad (8)$$

where μ is the renormalization point. The renormalization constant Z_3 depends on the renormalization prescription. We choose the momentum space subtraction (MOM) scheme where $Z_3(\mu^2, a)$ is determined by the tree-level value of the gluon propagator at the renormalization point, i.e.

$$D_R(q^2) \Big|_{q^2=\mu^2} = \frac{1}{\mu^2}. \quad (9)$$

In this study, we will choose to renormalize either at $\mu = 1$ or at $\mu = 4$ GeV.

IV. RESULTS

A. The effects of dynamical sea-quarks

To begin with, we discuss the effects of dynamical sea-quarks on the gluon propagator. First we compare the dressing function, $q^2 D(q^2)$, in full QCD to that

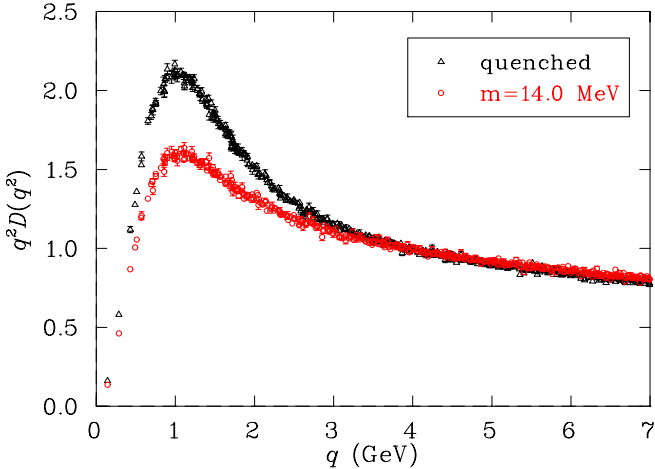


FIG. 1: Gluon dressing function in Landau gauge for the fine lattices ($28^3 \times 96$). Full triangles correspond to the quenched calculation, while open circles correspond to 2+1 flavor QCD. The bare light quark mass is $m = 14$ MeV for the full QCD result. As the lattice spacing and volume are the same, the difference between the two results is entirely due to the presence of quark loops. The renormalization point is at $\mu = 4$ GeV. Data has been cylinder cut [15].

in quenched QCD. For the fine lattices this is shown in Fig. 1. Obviously, the infrared hump seen in the quenched case is somewhat suppressed (about 30%) due to color screening by the quark-anti-quark pairs. The basic shape, however, is the same in the quenched and dynamical cases. This is consistent with previous results on smaller, coarser lattices [23] by some of us, and also with results obtained independently using clover-improved Wilson fermions [24, 25].

In Fig. 2 we are looking for the dependence of the dressing function on the sea quark mass. In this case the light quark masses differ by a factor of two (the strange quark has the same mass in both cases), but we see no effect. Note that in Ref. [23] a small quantitative difference has been observed by studying a slightly greater range of masses (the heaviest had four times the mass of the lightest). It would be interesting to study the gluon propagator with heavier sea quarks so that the transition between quenched and full QCD could be observed. We leave this for a future paper.

B. The scaling behavior

The renormalized propagator becomes independent of the lattice spacing as the continuum limit is approached. We can see this expected result in the renormalized quenched dressing function in Fig. 3. There data from the coarse and fine lattices are compared, having been renormalized at $\mu = 4$ GeV. These two sets of data almost lie on the same curve, and hence we conclude that good scaling is found for the quenched results.

Turning now to full QCD, in Fig. 4 we compare the

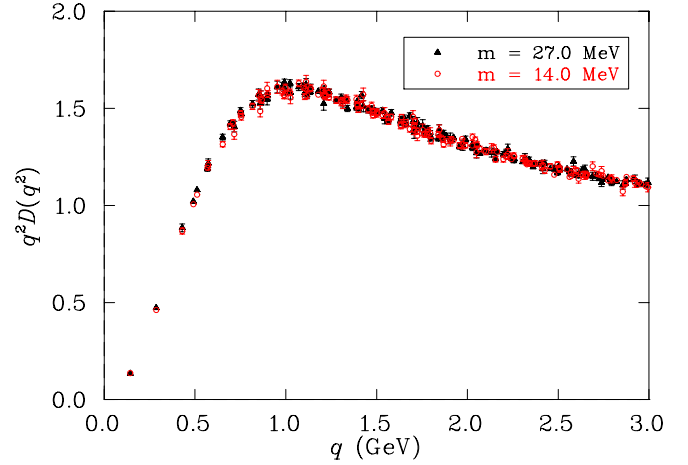


FIG. 2: The sea quark mass dependence of the Landau gauge gluon dressing function for the fine lattices. Filled triangles correspond to bare light quark mass $m = 27$ MeV, open circles correspond to the bare light quark mass $m = 14$ MeV. Data has been cylinder cut [15]. No mass dependence is observed for this case.

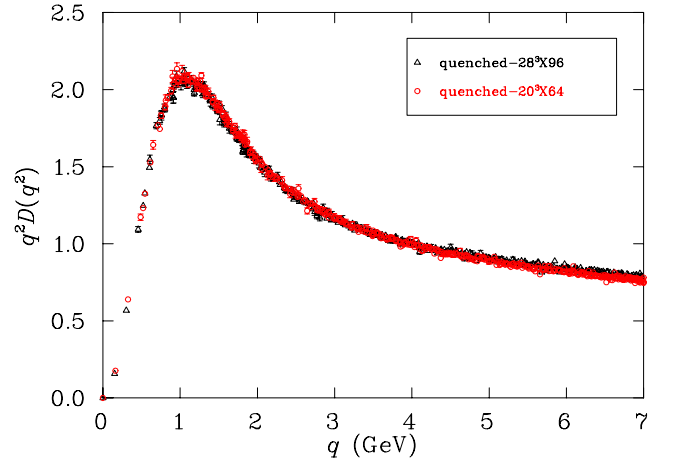


FIG. 3: The scaling behavior of the quenched gluon dressing function renormalized at $\mu = 4$ GeV. Triangles corresponds to the gluon propagator on the fine ensemble, open circles to the coarse ensemble. Good scaling is observed.

gluon dressing function from the fine ensemble for the lightest available sea quark mass (14 MeV) with that at an approximately equivalent quark mass from the coarse ensemble. Ideally while altering the lattice spacing we should hold the running quark mass (rather than bare quark mass) constant. The quark mass function was studied in Ref. [42] using these gauge configurations and it was found that a bare quark mass of 14 MeV on the fine ensemble had the same running mass as a bare quark of 11 MeV on the coarse ensemble. We therefore perform the small extrapolation of the coarse ensemble gluon propagator to 11 MeV for this comparison. Some very small systematic difference at the highest momenta is suggested, but this is where the discretization errors are

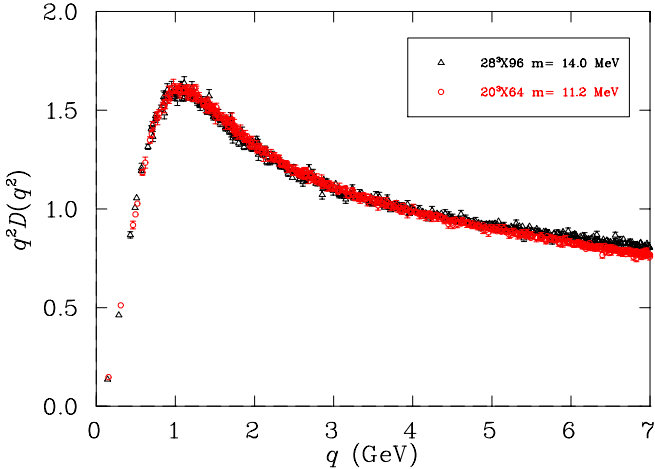


FIG. 4: The scaling behavior of the renormalized propagator in full QCD at $\mu = 4$ GeV. Triangles corresponds to gluon dressing function from the fine ensemble for sea quark mass $m = 14$ MeV. The open circles is for sea quark mass $m = 11$ MeV which is obtained by extrapolating the coarse ensemble data. Some difference is seen in the large momentum region.

TABLE II: Quenched configurations used in Ref. [13] listed in order of increasing volume. For this study the lattice spacing has been set using the string tension $\sqrt{\sigma} = 440$ MeV.

Dimensions	β	a (fm)	Action	#Config.
1	$16^3 \times 32$	4.38	0.165	Tree-level Symanzik
2	$32^3 \times 64$	6.00	0.0982	Wilson
3	$12^3 \times 24$	4.10	0.270	Tree-level Symanzik
4	$10^3 \times 20$	3.92	0.35	Tree-level Symanzik
5	$16^3 \times 32$	3.92	0.35	Tree-level Symanzik

expected to be large.

In the quenched case we can compare with a wider range of data sets. In Fig. 5 we include results from Ref. [13]. These were produced using the $\mathcal{O}(a^2)$ Symanzik tree-level improved gauge action, except for the $\beta = 6.0$ configurations which were generated with the single-plaquette Wilson gauge action. We renormalize at 1 GeV so as to accommodate the coarsest lattices. We use the string tension, $\sqrt{\sigma} = 440$ MeV, to set the lattice spacing. For $\beta = 6.0$ the precise measurement of Ref. [43] was used. A summary of these details is provided in Table. II. The three gauge actions approach the continuum limit slightly differently: for the tree-level improved gauge action the ultraviolet tail of the gluon propagator drops as the lattice spacing shrinks while for the one-loop improved action the tail rises. They do appear to be converging to the same result.

We also revisit the deep infrared region of the gluon propagator itself in Fig. 6. The $16^3 \times 32, \beta = 3.92$ lattice has by far the largest physical volume ($4.93^3 \times 9.86$ fm 4) and the smallest value for $D(q^2 = 0)$. The propagator

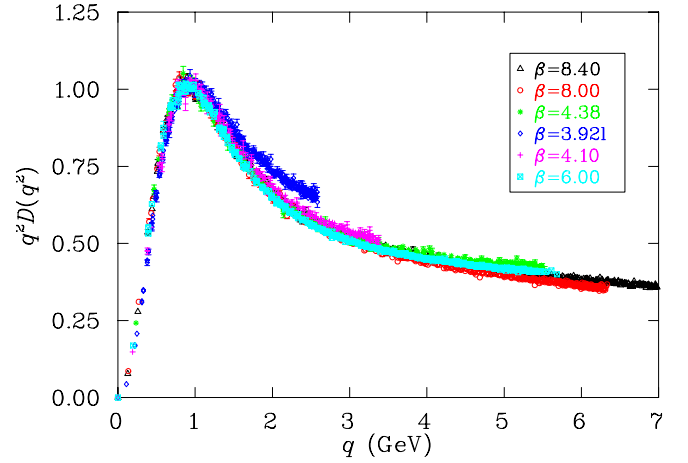


FIG. 5: The quenched gluon dressing function renormalized at 1 GeV using a variety of lattice spacings and gauge actions.

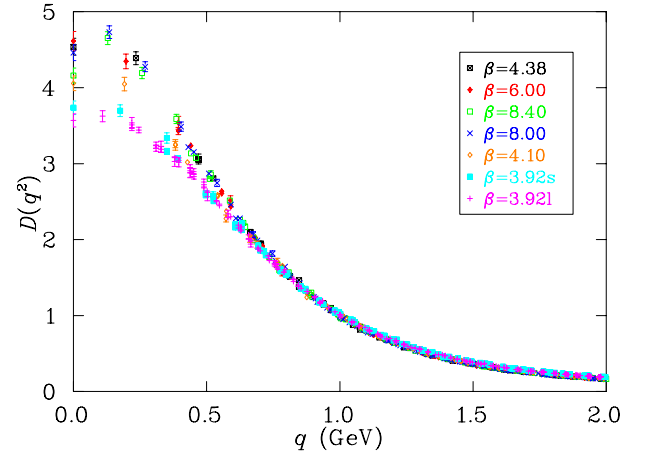


FIG. 6: The quenched gluon propagator renormalized at 1 GeV using a variety of lattice spacings and three different gauge actions. The value at zero four-momentum drops as the lattice volume increases.

systematically increases as the four-volume gets smaller. Finite volume effects are no longer significant for momenta above about 700 MeV.

C. Violation of reflection positivity

Now we turn to the Euclidean time correlator, Eq. (2). On the lattice this function can be evaluated using the discrete Fourier transform

$$C(t) = \frac{1}{\sqrt{L_4}} \sum_{n_4=0}^{L_4-1} e^{-2\pi i n_4 t / L_4} D(p_4, 0), \quad (10)$$

where L_4 is the number of lattice points in time direction, p_4 is the Euclidean time component of the lattice momentum, n_4 is an integer and $D(p_4, 0)$ is the gluon

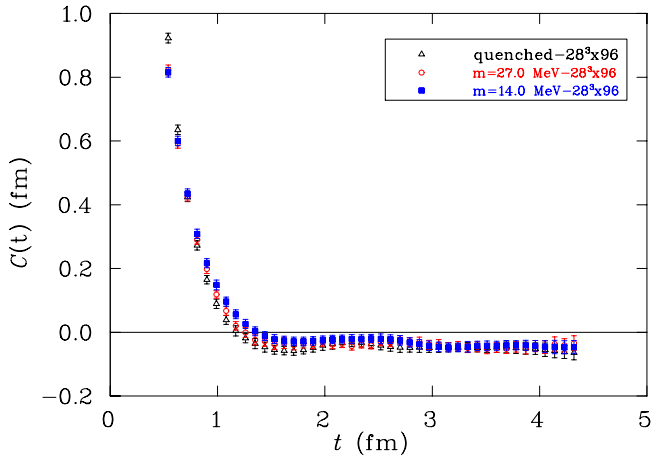


FIG. 7: The real space propagator $C(t)$ for $28^3 \times 96$ lattices plotted as a function of dimensionful t for both light sea quark masses and the quenched case. Reflection positivity is clearly violated in all three cases.

propagator in momentum space at zero spatial momentum.

In Fig. 7, $C(t)$ is shown for the fine lattices in the quenched case and for both choices of sea quark. In all cases the Schwinger function clearly becomes negative signaling explicit reflection-positivity violation by the gluon propagator.

At large Euclidean time, $C(t)$ is expected to reach zero from below. Unfortunately, this cannot be seen from our data shown in Fig. 7. Something similar has been observed independently using a different fermion formulation [26]. The reason might be the difference in the number of lattice points in spatial and temporal directions. It is known [16] that on an asymmetric lattice the gluon propagator can violate the infinite-volume continuum-limit tensor structure (Eq. (3)) in the (extended) time direction at very low momentum values. As is customary, we assumed the continuum tensor structure and thus $D(p=0)$ has been normalized by $N_d = 4$ and $D(p>0)$ by $N_d - 1 = 3$. However, using a slightly different normalization either for $D(0)$ or $D(p>0)$ the data in Fig. 7 could be easily shifted towards larger values such that (within errors) they equal zero at large t . This suggests the more general form for the Landau-gauge gluon propagator [16]

$$D_{\mu\nu}^{ab}(q) = \left(\delta_{\mu\nu} - \frac{h_{\mu\nu}(q)}{f(q^2)} \right) \delta^{ab} D(q^2) \quad (11)$$

might be more appropriate. Here $f(q^2) \rightarrow q^2$ and $h_{\mu\nu} \rightarrow q_\mu q_\nu$ for sufficiently large q , but are generally unknown and go to finite values for $q = 0$.

Apart from $C(t)$, it is also interesting to consider its absolute value and to compare our lattice data with corresponding DSE results by Alkofer *et al.* [32]. Those results have been reprinted on the right-hand side of Fig. 8. On the left-hand side we present our lattice result for $|C(t)|$ on the fine ensemble. The two figures are remarkably alike: not only does the zero crossing occur at almost the same place in Euclidean time, $t \approx 5 \text{ GeV}^{-1}$ (about the size of a hadron), but the DSE results also correctly predict the small shift due to the inclusion of dynamical quarks. This shift is largest in our data for the smallest light quark mass. A similar result is obtained by using the coarse lattices.

V. CONCLUSIONS

We have extended a previous lattice study [23] of the Landau-gauge gluon propagator in full QCD to a finer lattice. The addition of quark loops has a clear, quantitative effect on the gluon propagator, but its basic features are unaltered. Good scaling behavior is observed for the gluon dressing function in both the quenched and unquenched cases with these improved actions.

The violation of reflection positivity of the gluon propagator was investigated by calculating the real space propagator, or Schwinger function; the Landau gauge gluon propagator clearly violates positivity in both quenched and full QCD.

ACKNOWLEDGMENTS

This research was supported by the Australian Research Council and by grants of time on the Hydra Supercomputer, supported by the South Australian Partnership for Advanced Computing. We thank the MILC Collaboration for providing the results of their static quark potential measurements. J. B. Zhang is supported by Chinese national natural science foundation grant 10675101.

[1] R. Alkofer and L. von Smekal, Phys. Rept. **353**, 281 (2001), hep-ph/0007355.
[2] C. D. Roberts and A. G. Williams, Prog. Part. Nucl. Phys. **33**, 477 (1994), hep-ph/9403224.
[3] C. D. Roberts and S. M. Schmidt, Prog. Part. Nucl. Phys. **45**, S1 (2000), nucl-th/0005064.
[4] P. Maris and C. D. Roberts, Int. J. Mod. Phys. **E12**, 297 (2003), nucl-th/0301049.
[5] A. Höll, C. D. Roberts, and S. V. Wright (2006), nucl-th/0601071.
[6] J. E. Mandula and M. Ogilvie, Phys. Lett. **B185**, 127 (1987).

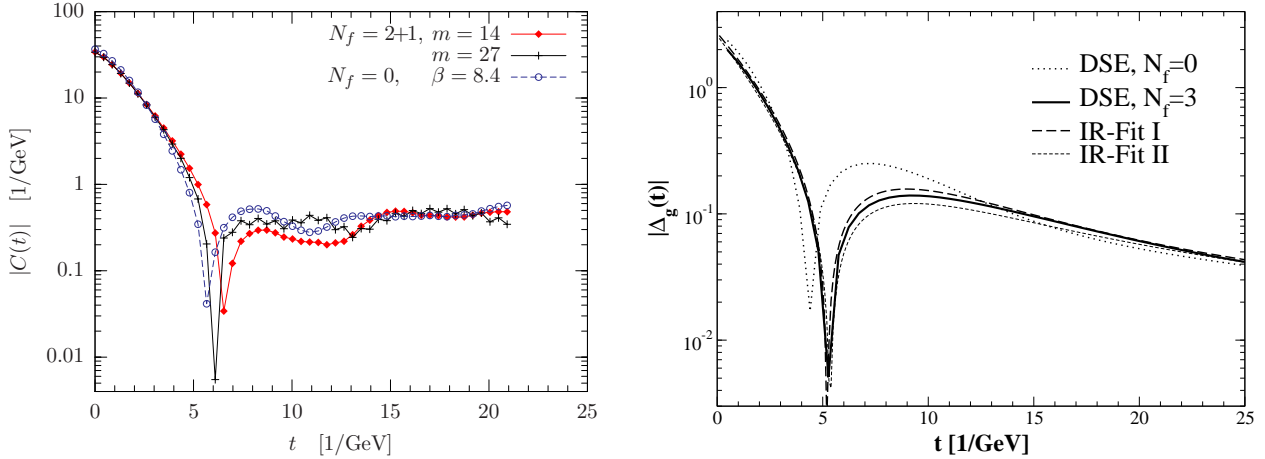


FIG. 8: The left figure corresponds to the absolute value of the gluon Schwinger function from our fine lattice calculations in quenched QCD as well as in full QCD. Error bars are not shown for simplicity. The bare quark masses for full QCD simulations are $m = 27$ MeV and $m = 14$ MeV, respectively. The right figure is taken from [32]. It shows the numerical results for the absolute value of the Schwinger function from the DSE result compared to the fits in the infrared. See Ref. [32] for more details.

- [7] C. W. Bernard, C. Parrinello, and A. Soni, Phys. Rev. **D49**, 1585 (1994), hep-lat/9307001.
- [8] P. Marenzoni, G. Martinelli, and N. Stella, Nucl. Phys. **B455**, 339 (1995), hep-lat/9410011.
- [9] J. P. Ma, Mod. Phys. Lett. **A15**, 229 (2000), hep-lat/9903009.
- [10] D. Becirevic et al., Phys. Rev. **D60**, 094509 (1999), hep-ph/9903364.
- [11] D. Becirevic et al., Phys. Rev. **D61**, 114508 (2000), hep-ph/9910204.
- [12] H. Nakajima and S. Furui, Nucl. Phys. **A680**, 151 (2000), hep-lat/0004023.
- [13] F. D. R. Bonnet, P. O. Bowman, D. B. Leinweber, A. G. Williams, and J. M. Zanotti, Phys. Rev. **D64**, 034501 (2001), hep-lat/0101013.
- [14] K. Langfeld, H. Reinhardt, and J. Gattnar, Nucl. Phys. **B621**, 131 (2002), hep-ph/0107141.
- [15] D. B. Leinweber, J. I. Skullerud, A. G. Williams, and C. Parrinello, Phys. Rev. **D60**, 094507 (1999), hep-lat/9811027.
- [16] D. B. Leinweber, J. I. Skullerud, A. G. Williams, and C. Parrinello, Phys. Rev. **D58**, 031501 (1998), hep-lat/9803015.
- [17] F. D. R. Bonnet, P. O. Bowman, D. B. Leinweber, and A. G. Williams, Phys. Rev. **D62**, 051501 (2000), hep-lat/0002020.
- [18] A. Sternbeck, E.-M. Ilgenfritz, M. Müller-Preussker, and A. Schiller, Phys. Rev. **D72**, 014507 (2005), hep-lat/0506007.
- [19] P. J. Silva and O. Oliveira, Phys. Rev. **D74**, 034513 (2006), hep-lat/0511043.
- [20] J. C. R. Bloch, A. Cucchieri, K. Langfeld, and T. Mendes, Nucl. Phys. **B687**, 76 (2004), hep-lat/0312036.
- [21] A. Cucchieri, Phys. Lett. **B422**, 233 (1998), hep-lat/9709015.
- [22] A. Cucchieri, T. Mendes, and A. R. Taurines, Phys. Rev. **D67**, 091502 (2003), hep-lat/0302022.
- [23] P. O. Bowman, U. M. Heller, D. B. Leinweber, M. B. Parappilly, and A. G. Williams, Phys. Rev. **D70**, 034509 (2004), hep-lat/0402032.
- [24] A. Sternbeck, Ph.D. thesis, Humboldt-University Berlin (2006), hep-lat/0609016.
- [25] E.-M. Ilgenfritz, M. Müller-Preussker, A. Sternbeck, A. Schiller, and I. L. Bogolubsky (2006), to appear in Brazilian Journal of Physics, hep-lat/0609043.
- [26] A. Sternbeck, E.-M. Ilgenfritz, M. Müller-Preussker, A. Schiller, and I. L. Bogolubsky, PoS **LAT2006**, 076 (2006), hep-lat/0610053.
- [27] L. von Smekal, R. Alkofer, and A. Hauck, Phys. Rev. Lett. **79**, 3591 (1997), hep-ph/9705242.
- [28] L. von Smekal, A. Hauck, and R. Alkofer, Ann. Phys. **267**, 1 (1998), hep-ph/9707327.
- [29] D. Zwanziger, Phys. Rev. **D65**, 094039 (2002), hep-th/0109224.
- [30] J. M. Pawłowski, D. F. Litim, S. Nedelko, and L. von Smekal, Phys. Rev. Lett. **93**, 152002 (2004), hep-th/0312324.
- [31] C. S. Fischer, A. Maas, J. M. Pawłowski, and L. von Smekal (2007), hep-ph/0701050.
- [32] R. Alkofer, W. Detmold, C. S. Fischer, and P. Maris, Phys. Rev. **D70**, 014014 (2004), hep-ph/0309077.
- [33] C. A. Aubin and M. C. Ogilvie, Phys. Lett. **B570**, 59 (2003), hep-lat/0306012.
- [34] C. W. Bernard, C. Parrinello, and A. Soni, Nucl. Phys. Proc. Suppl. **30**, 535 (1993), hep-lat/9211020.
- [35] P. Marenzoni, G. Martinelli, N. Stella, and M. Testa, Phys. Lett. **B318**, 511 (1993).
- [36] H. Aiso et al., Nucl. Phys. Proc. Suppl. **53**, 570 (1997).
- [37] A. Cucchieri, T. Mendes, and A. R. Taurines, Phys. Rev. **D71**, 051902 (2005), hep-lat/0406020.
- [38] S. Furui and H. Nakajima (2004), hep-lat/0403021.
- [39] C. Aubin et al., Phys. Rev. **D70**, 094505 (2004), hep-lat/0402030.
- [40] NERSC, *Gauge connection*, <http://qcd.nersc.gov/>.
- [41] M. Lüscher and P. Weisz, Commun. Math. Phys. **97**, 59 (1985).
- [42] M. B. Parappilly et al., Phys. Rev. **D73**, 054504 (2006), hep-lat/0511007.
- [43] R. G. Edwards, U. M. Heller, and T. R. Klassen, Nucl. Phys. **B517**, 377 (1998), hep-lat/9711003.